Quantitative risk analysis of gas explosions in tunnels

Weerheijm, J.; Verreault, J.; van der Voort, M. M.

DOI
10.1016/j.firesaf.2017.06.003

Publication date
2018

Document Version
Accepted author manuscript

Published in
Fire Safety Journal

Postprint of Marine Geology
Available online 18 July 2017
Link to formal publication (Elsevier): https://doi.org/10.1016/j.firesaf.2017.06.003

Quantitative risk analysis of gas explosions in tunnels

J. Weerheijm1[1,2], J. Verreault[1], M.M. van der Voort[3]
[1]TNO, Lange Kleiweg 137, 2280 AA Rijswijk, The Netherlands
[2]University of Technology Delft, Faculty of Civil Engineering
[3]Munitions Safety Information Analysis Center (NATO), B 1550, BZ S054, B-1110, Brussels, Belgium

ABSTRACT

Transportation of flammable liquefied gas in tunnels presents a significant risk of an accidental loss of containment leading to an explosion with major consequences. Possible scenarios include a BLEVE, a non-reactive gas expansion explosion and a reactive gas explosion. Quantification of the risk and consequences associated with such events is central in the design of tunnels and routing of dangerous goods. TNO previously developed a Quantitative Risk Analysis (QRA) method, which combines a probability assessment with state-of-the-art explosion effect and consequence models [16]. This article extends this model to combine the dispersion of a flammable cloud with its probability of ignition and the resulting physical effects such as overpressure. The model assumes an increasing probability of ignition with both the number and the duration of vehicles present within the flammable cloud. Various case studies are considered to illustrate the effect of different ignition probability parameters. These cases deal with instantaneous and continuous LPG releases with varying release rates including the effect of ventilation. They clearly show the capability to quantify the gas explosion load and ignition probabilities. The combination of the gas dispersion, gas explosion and ignition probability models are needed to derive design loads for tunnels, to perform tunnel safety assessments, and to develop safety measures. These models form the backbone for quantitative risk assessments.

KEYWORD: explosion, tunnel design, probability, risks, models, transport dangerous goods.

1 INTRODUCTION

Tunnel accidents with transports of flammable liquefied gases may lead to loss of containment and explosions. Depending on the substance involved this can be a Boiling Liquid Expanding Vapour Explosion (BLEVE), a Gas Expansion Explosion (GEE, a non-reactive explosion due to the rapid expansion of the gas) or a gas explosion (a deflagration or detonation). The relevance of gas explosions in road tunnels was recently confirmed by two major accidents. An accident with a liquefied natural gas tanker in central China in 2012 killed five people. In Bremanger (Norway) a gasoline fuel truck crashed into the side walls of an undersea tunnel in July 2015. This triggered a series of explosions that even caused leakage of seawater into the tunnel and fear of collapse. Quantification of the risk of these scenarios is important to take informed decisions on tunnel design and routing of dangerous goods.

Weerheijm and Van den Berg [16] presented the background of tunnel explosion safety research and modelling in the Netherlands related to transport of flammable liquefied gases. They provided an overview of various numerical models developed to assess the overpressure effects of BLEVE, GEE,

1 Corresponding author: jaap.weerheijm@tno.nl

and gas explosions, and their application to case studies. More detail can be found in other references [1, 2, 3, 5, 10].

This study aims at showing the capability of assessing the ignition probability of gas explosion scenarios in road tunnels as well as evaluating the resulting physical effects such as overpressure. A first outline of this approach was described in [14] and [17]. While models for dispersion of gas and subsequent explosion have been developed by others and TNO [2, 13, 15, 18] the current investigation combines a dispersion model with the probability of ignition of the combustible cloud and the resulting physical effects, as shown in Figure 1.1. Therefore this study describes a model capable to provide a quantitative risk analysis.

Section 2 describes the gas explosion mechanism, and models for gas dispersion and gas explosion. This introduces the key parameters for the explosion load in a tunnel. Section 3 presents an integrated model for the dispersion and probability of ignition. Three case studies are then presented in Section 4 to show the capability to quantify the gas explosion load and probabilities for various accident scenarios. The input data for these case studies is based on tunnel and transport data in the Netherlands. Furthermore the transport of LPG (Liquefied Propane Gas) is considered since it is most relevant for tunnel safety in The Netherlands and it can potentially generate all explosion types.

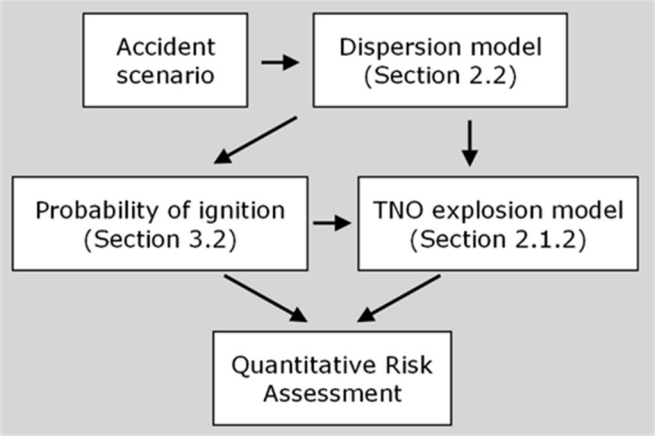

Figure 1.1 Links between the different models required for a quantitative risk assessment.

2 MODEL DESCRIPTION

2.1 Gas explosion

2.1.1 Explosion mechanism

A mixture of a fuel and air can only be ignited when its composition is between its lower flammability limit (LFL) and upper flammability limit (UFL). For a propane-air mixture the fuel gas concentration must be between 2 and 9%. Such a mixture is called an explosive mixture. When the mixture ignites, for instance by a spark or a hot surface, a flame front starts propagating into the reactive mixture. The flame propagates due to the transport of heat. Heat is produced in the combustion reaction in the flame front, the flame sheet is transported into the unburned mixture ahead of the flame by molecular transport processes such as conduction and diffusion of heat and species. In this way the mixture in front of the reaction zone is heated up to ignition whereupon it starts to react.

The chemical reaction produces combustion products at a high temperature. Because of the large temperature increase (more than 2000 K for HC(hydrogen-carbon)-air mixtures) the gases expand severely. The expansion generates a flow field in which the flame front is carried along. Relative to

the unburned mixture (which is almost always in motion by the expansion), the flame front propagates at the laminar burning speed initially. When a flame propagates into a gas mixture that is in turbulent motion, the flame sheet gets distorted. The vorticity of the turbulence deforms the flame sheet and enlarges its reactive surface area thereby. Under the influence of intense turbulence, the flame velocity may increase up to many times the initial laminar burning velocity. The basic mechanism of flame sheet propagation however, is still based on the transport of heat and species and is called a deflagration.

A deflagration process intensifies if the flame propagation process can generate its own turbulence in interaction with the boundary conditions for the flow field. For a tunnel tube the walls and the cars will determine the turbulence conditions. The turbulence affects the flame front and increases its burning speed. An increased burning speed intensifies the expansion flow and its turbulence level, which subsequently increases the flame speed further to initiate a run-away process. In this way the geometrical boundary conditions trigger a feed-back coupling in the flame propagation process. The feed-back coupling continuously intensifies the flame propagation process both in speed and pressure. This Schelkin effect [12] has been illustrated in Figure 2-1

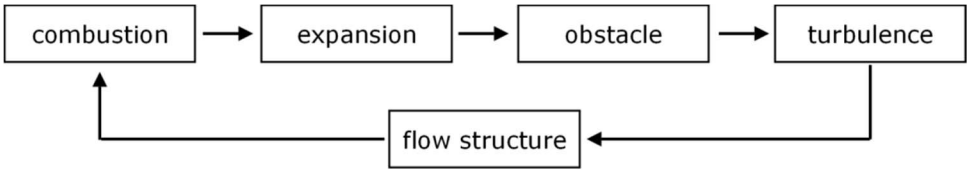

Figure 2.1 The Schelkin effect- The feed back coupling in the process of flame propagation through the boundary conditions.

In empty tubes of sufficient length (many tens of tube diameters), flame propagation in HC-air mixtures may develop a propagation velocity of many hundreds of meters per second and an overpressure of several bars. When the chemical reaction intensifies, the pressure and temperature at the reaction front increases to levels of self-ignition, a deflagration process may suddenly change its propagation mode and transition to detonation. Due to the range of possible deflagration scenarios (from laminar to highly turbulent), the resulting pressure can vary between 10 kPa and 800 kPa for HC-air mixtures. When the gas explosion intensifies to pressures in the order of 800 kPa the deflagration –detonation transition (DDT) may occur.

In a detonation the flame propagates with a leading strong shock wave. The shock wave compresses the reactive mixture far beyond its auto-ignition temperature whereupon a combustion reaction wave couples to the shock wave. The energy released by the combustion maintains the propagation of the shock wave while the shock wave triggers the combustion reaction. A detonation is supersonic and for HC-air mixtures explosion loads are in the order of 1500-2000 kPa. For a thorough description of the gas explosion mechanism see [2, 3, 16].

2.1.2 TNO explosion model

Modeling of a gas explosion is a challenging tasks due to complex physical processes involving reactive gas dynamics and computational fluid dynamics. Furthermore these processes occur at a wide range of timescales (10^{-6} to 1 s) and length scales (10^{-4} – 10^{1} m) which makes them impractical to model in detail. The TNO explosion model is a fast-running tool that was developed using a combination of small-scale tunnel experiments with representative obstacle arrays and a 1D CFD gas explosion code, as shown in Figure 2-2. A brief description of the CFD code is provided in Annex A.

The TNO explosion model therefore keeps certain aspects of the CFD code (although largely simplified) while being calibrated using the small-scale experiments in order to account for complex phenomena such as turbulence. This model is thus suitable to be used as input for QRA's.

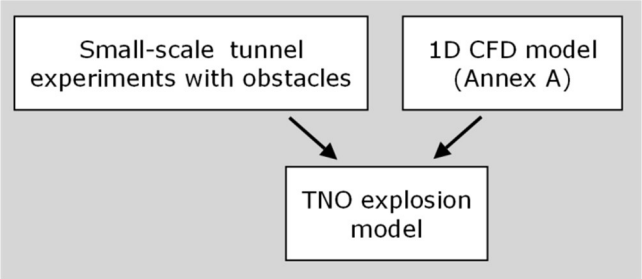

Figure 2.2 The TNO explosion model was developed using a combination of small-scale experiments and a CFD model.

As mentioned in Section 2.1.1, pressure loads are related to flammable cloud lengths. In [1] guidelines for the explosion load as a function of the cloud length with a stoichiometric concentration were compiled. The guidelines have been drawn up by using the highly simplified model for the gas dynamics of a gas explosion in a tube [1, 10, 11]. The current paper considers scenarios in which the explosive mixture ignites as soon as it meets a stationary ignition source. The maximum pressure loads dependent on cloud lengths have been tabulated in Table 2.1. Note, that for cloud lengths larger than 50 m the explosion pressure load rapidly increases up to 800 kPa and the deflagration to detonation transition might occur, depending on various factors such as the tunnel cross section dimensions. In the current paper a critical length of about 80 m is assumed.

Table 2.1 Explosion pressure load$ on the tunnel lining dependent on explosive cloud lengths for propane-air mixtures [2].

explosive cloud length (m)	explosion pressure load (kPa)	explosion pressure impulse (kPa.s)	relative rise time β#
2	13	1.9	1
4	32	4.9	0.6
6	47	7.1	0.5
8	65	9.4	0.5
10	83	11.5	0.4
20	190	21.2	0.2
30	340	28.8	0.1

40	500	36.3	0.1
50	700	>60@	<0.1
60	900	…	<0.1

β is the ratio of the pressure rise time and the positive phase duration of the explosion pressure
$ In this paper the explosion load, the "overpressure", is the load acting on the tunnel structure.
@ In the transition regime from deflagration to detonation the simulated pressure-time profile is very irregular and impulse data cannot be derived reliably.

2.2 Dispersion model

When the gas is released, initially the concentration varies over the cross section of the tunnel. Downwind, in the direction of the ventilation flow, the gas concentration becomes uniformly distributed over the cross section and can eventually be considered as one-dimentional. The one-dimensional dispersion model of Taylor [13] has been incorporated in the TNO model to determine the concentration distribution of the gas as a function of time and distance from the release point. Calculations can be made for instantaneous release of gas as well as for different continuous release rates. A detailed description of the model is given in [3] and Annex B.

Figure 2.3 shows the concentration distribution at consecutive points in time after an instantaneous release of 500 m^3 propane gas. It shows how the concentration gradually falls relative to the flammability region of propane in air. Initially, two areas of a flammable composition on both sides of the cloud are separated by an area of a composition too rich to be able to propagate a flame. Subsequently, when the maximum concentration falls below the upper flammability limit, there is one continuous area of a flammable composition.

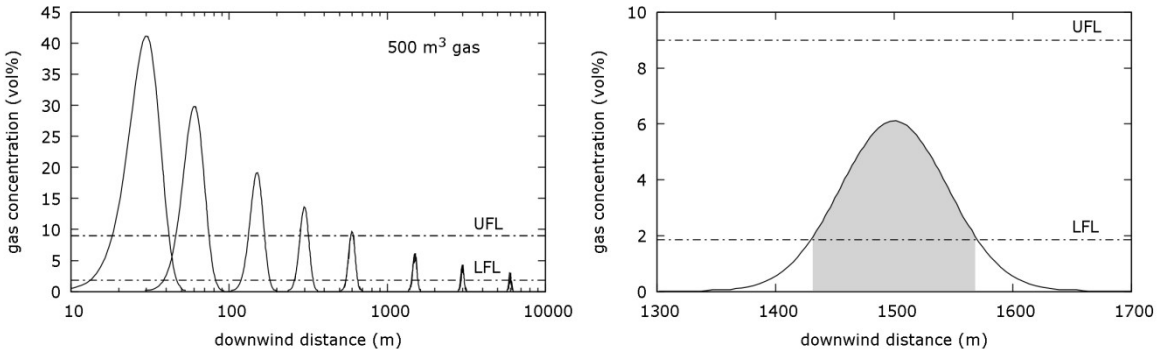

Figure 2.3 (Left) Concentration distributions downwind of an instantaneous release of 500 m^3 propane gas in a long tunnel tube after 10, 20, 50, 100, 200, 500, 1000, 2000 and 5000 s; (right) Concentration distribution downwind of a release of 500 m^3 propane after 500 s.

When gas is released from a continuous leak, and dispersed in a steady ventilation flow, the downwind concentration is constant and equal to:

$$C = \frac{Q}{\rho.U.A_t} \times 100\% \qquad (1)$$

where: C = steady downwind concentration ($m^3.m^{-3}$); Q = leak rate ($kg.s^{-1}$); ρ = propane vapour density (1.9 $kg.m^{-3}$); U = ventilation wind speed ($m.s^{-1}$) and A_t = tunnel cross-sectional area (m^2) This dispersion model allows the determination of an explosive cloud length as a function of release rate and tunnel conditions, which is shown inFigure 2.4. This figure also shows the cloud length threshold of about 50 meters (seeTable 2.1) above which DDT might occur.

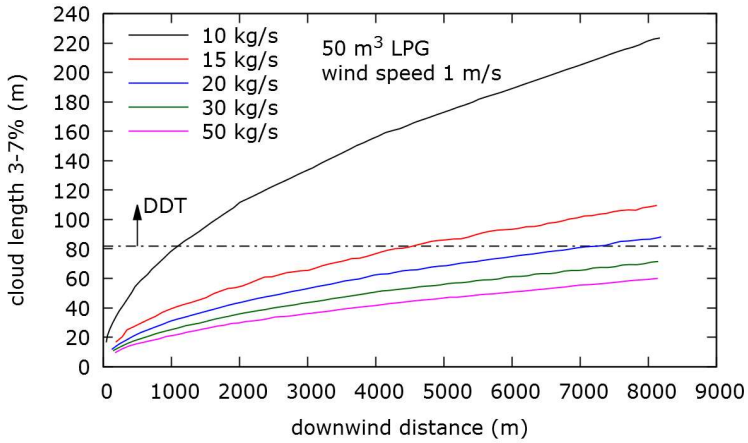

Figure 2.4 Downwind explosive cloud length development for various leak rates in a tunnel of 5×14.4 m² cross-sectional area and a 1 m/s ventilation wind speed [3].

3 INTEGRATION OF MODELS FOR DISPERSION AND PROBABILITY OF IGNITION

3.1 Problem definition and assumptions

A tunnel with length L_T is considered as shown inFigure 3-1. Distances in the tunnel are measured on an x-axis with its origin at the left tunnel exit. In the tunnel a ventilation speed U_v is present in the direction of the traffic. The number of vehicles per meter is given by the linear density ρ(x,t) expressed in cars/m.

At location x = x_{C0} and time t = 0 an accident takes place with a truck transporting a flammable liquefied gas. From t = 0 onwards a leakage results in a cloud that mixes with air and moves downstream. Both instantaneous and continuous release scenarios are considered, followed by direct or delayed ingnition. Depending on the gas concentration at a given time and location, the cloud can either be flammable (between the LFL and the UFL) or non-flammable (below the LFL or above the UFL).

Figure 3.1 Schematic of the considered scenario where an accident is caused by a truck at position x_{c0} in a traffic jam.

For propane-air mixtures the auto-ignition temperature is 470 °C [11], and the Minimum Ignition Energy (MIE) is between 0.25 mJ [9] and 0.46 mJ [5]. The auto-ignition temperature is usually not reached in an ordinary combustion engine, but a static discharge easily exceeds the MIE. As a result the most realistic option for an ignition is a static discharge generated by vehicles. Therefore it is assumed that a possible ignition of the combustibe cloud is dominated by the vehicles.

In brief it is assumed that the ventilation speed is in the direction of the traffic, and that the ignition probability is dominated by vehicles. These assumptions imply that the accident scenario of a truck driving into a traffic jam is the most relevant to consider for this study. In this case the explosive cloud will potentially meet a large number of vehicles (ignition sources). The scenario in which the traffic dilutes in front of the accident would yield a small (if not zero) ignition probability, and is not considered here.

3.2 Probability of ignition

This section describes the model which combines the dispersion of a flammable cloud with its probability of ignition. A typical gas concentration profile is presented inFigure 3-2. This figure also shows the LFL and the UFL of a propane-air mixture at atmospheric pressure. Flammable clouds are thus defined where the gas concentration is between the flammability limits. Considering a ventilation direction downstream, the length of the leading and trailing flammable clouds are defined as $L_{leading}$ and $L_{trailing}$, respectively. The total flammable cloud length (L) is therefore: $L = L_{leading} + L_{trailing}$. As the maximum gas concentration decreases downstream, it is also possible that the leading and trailing flammable cloud merge into a single cloud with length L.

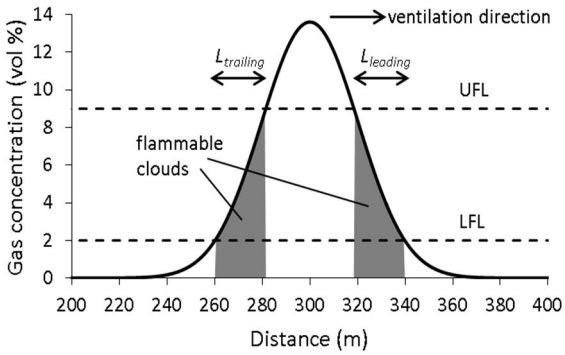

Figure 3.2 Typical gas concentration profile including the LFL, the UFL and the definition of flammable clouds.

Considering a constant car density ρ in the tunnel we can calculate the number of cars in the flammable cloud(s) as follows:

$$n = n_{leading} + n_{traling} \quad (2)$$

$$n_{leading} = \rho \cdot L_{leading} \quad (3)$$

$$n_{trailing} = \rho \cdot L_{trailing} \quad (4)$$

n: number of cars (cars)

ρ: car density (cars/m)

Defining the ignition probability caused by a single car which remains in a flammable mixture for one second as $P_{single\ car}$, the ignition probability for a given gas concentration profile is obtained by using the so-called power-up rule for the leading and trailing flammable clouds:

$$P_{j,leading} = 1 - \left(1 - P_{single\ car}\right)^{n_{leading}} \quad (5)$$

$$P_{j,trailing} = 1 - \left(1 - P_{single\ car}\right)^{n_{trailing}} \quad (6)$$

With $P_{j,leading}$: ignition probability of the leading flammable cloud for one time step at time t_j

and $P_{j,trailing}$: ignition probability of the trailing flammable cloud for one time step at time t_j

In the above relation, it is important that the time step used in the simulation corresponds to the definition of $P_{single\ car}$,, which is in this case one second. To obtain the overall ignition probability at time t_j including the two flammable clouds the following relation is used:

$$P_j = 1 - \left(1 - P_{j,leading}\right)\left(1 - P_{j,trailing}\right) \quad (7)$$

With P_j: ignition probability for one time step at time t_j

In case the two flammable clouds merge into a single flammable cloud the ignition probability is expressed as:

$$P_j = 1 - \left(1 - P_{single\ car}\right)^n \quad (8)$$

As the cloud travels along the tunnel, the ignition probability at consecutive time steps must be cumulated. The cumulative ignition probability is hence obtained with the following relation:

$$P_{cumul} = 1 - \prod_{j=1}^{m}\left(1 - P_j\right) \quad (9)$$

with m: number of time steps andP_{cumul}: cumulative ignition probability

The mathematical form of this relation differs from the previous one because P_j varies at each time step. The cumulative ignition probability provides the probability that the flammable cloud ignite before a given time. In a risk analysis it is of interest to define a representative set of scenarios with their respective probability of occurrence, physical effects, and consequences. In this case, a scenario corresponds to an ignition within a certain time interval (i.e. for a certain flammable cloud length). The probability of the different scenarios is obtained using the cumulative probability versus time:

$$P_{scenario} = P_{cumul}(t + \Delta t) - P_{cumul}(t) \quad (10)$$

With $P_{scenario}$: ignition probability at a given time

Note that Δt may be but is not necessarily equal to the time step used in the dispersion and cumulative probability calculation. Also, the Probability Density Function (PDF) is of interest as it can be used to determine some interesting statistical parameters, such as the mode and arithmetic mean.

$$P_{PDF} = \frac{dP_{cumul}}{dt}$$

With P_{PDF}: probability density function

An example of a probability density function is shown in Figure 3.3 with an illustration of the mode, median and mean values. The mode corresponds to the scenario that occurs the most often (maximum of the function). The median refers to the point where half of the scenarios has occurred (where the area under the curve is separated into half). The arithmetic mean is the scenario that occurs on average (sum of the scenario probability divided by the total number of scenarios).

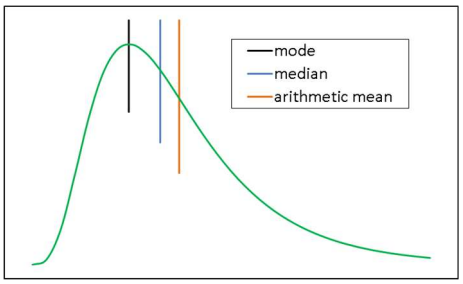

Figure 3.3 Illustration of the mode(line-left), median(line-middle) and mean (line –right) of a probability density function.

Additionally the following aspects are taken into account:

- After the explosive cloud has reached a location, some time is needed for the flammable gas to disperse into or below a vehicle and to allow ignition to take place. This dispersion time is accounted for using a delay time t_d.
- Outside the tunnel ($x < 0$, of $x > L_T$) the cloud quickly dilutes and is therefore discarded from the calculation of the ignition probability.

4 CASE STUDIES

4.1 Introduction

Different cases are considered to illustrate the calculation procedure and the resulting ignition probability of a flammable mixture and the corresponding overpressure in a tunnel for a given accident. The considered cases are introduced in Table 4.1 and the parameters are divided into two categories: the dispersion and probability parameters.
Case 1 refers to an 80% filled 60 m^3 LPG tank, from which 50 m^3 of LPG is instantaneously released. A flash fraction of 0.5 is assumed which can be derived by calculating the temperature fall of the liquid down to the saturation temperature at the reduced pressure using temperature-dependent heat of evaporation and specific heat. Assuming an expansion ratio of 260, the gaseous fuel volume is 6500 m^3 which is then free to disperse in the tunnel. Case 2 refers to a nearly empty (1% filled) tank of LPG at its vapour pressure of 730 kPa (at a temperature of 288 K). In this case the volume of the evaporated gas (expanded to ambient pressure) is 438 m^3. Case 3 refers to the situation where the 60 m^3 LPG tank ruptures partially and the LPG leaks out at a rate of 30 kg/s. Assuming a flash fraction of 0.5 the leaking rate of the gaseous fuel is 15 kg/s until the complete amount of LPG has leaked out.

Table 4.1 Parameters considered for the three cases.

	Parameters	Case 1	Case 2	Case 3
Dispersion parameters	Release type	instantaneous	instantaneous	continuous
	Volume of fuel (m^3 gas at ambient conditions)	6500	438	N/A
	Mass of LPG (kg)	N/A	N/A	12 500
	Density of gas fuel (kg/m^3)	N/A	N/A	1.9
	LPG leak rate (kg/s)	N/A	N/A	30
	Ventilation velocity (m/s)	2	2	2
	Tunnel cross section (m)	5 x 14.4	5 x 14.4	5 x 14.4
	Tunnel length (m)	1000	1000	1000
Probability parameters	Car density (cars/m)	0.05#	0.05	0.05
	Probability of a single car*	0.001, 0.007	0.001, 0.007	0.001, 0.007

Ignition delay (s)	5	5	5

* The ignition probability of a single car which remains in a flammable mixture for one second.
# Arbitrary value

The tunnel size has a cross section of 14.4 m x 5 m and a length of 1 km. The accident takes place at the entrance of the tunnel. A ventilation speed of 2 m/s is considered in the direction of the traffic. The probability parameters are identical for the three cases. A car density of 0.05 car/m (or 5 cars / 100 m) is considered. $P_{single\ car}$ is defined as the probability of ignition caused by a single car which remains in a flammable mixture for one second. For the case studie two arbitrary values are considered: 0.001 and 0.007. The same holds for the ignition delay which has been set at 5 s, which implies that the probability of ignition during this time is null. Note that no quantitative data is available on the ignition probability for a single car. Therefore values of 0.001 and 0.007 provide a qualitative comparison between a lower and a higher probability, as well as to demonstrate the capability to quantify ignition probabilities resulting from accident scenarios.

The simulation results for the three cases are presented in the following sections. The results consist of the evolution of the gas concentration profile until the cloud exits the tunnel, the flammable cloud length and position, the overpressure in case of ignition, the cumulative ignition probability of the flammable cloud and the ignition probability density function.

4.2 Results Case 1 and Case 2

In this section Cases 1 and 2 are presented and discussed in parallel to highlight the differences. The gas concentration profiles at different times after the rupture of the tank are displayed in **Error! Reference source not found.** . In this figure the UFL and LFL are also shown as dashed lines. Due to the large amount of fuel released in Case 1, most of the mixture concentration remains above the UFL until it reaches the exit of the tunnel. At any given time, there are therefore two flammable clouds (leading and trailing clouds) where the gas concentration is between the LFL and UFL. For Case 2 only initially there are two flammable clouds, but they merge quickly and a long explosive cloud is formed.

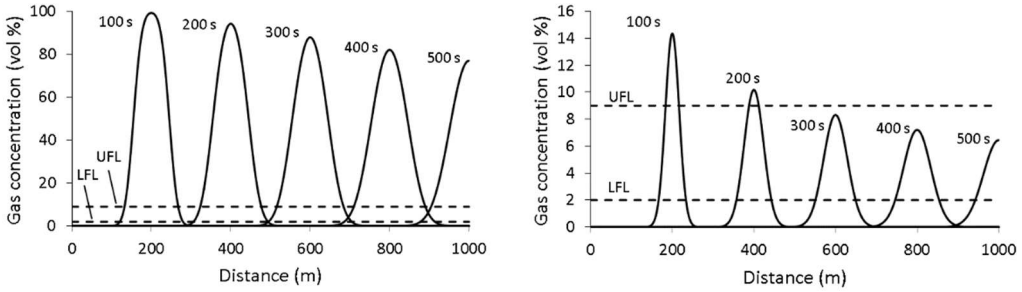

Figure 4.1 Gas concentration profiles at different times. Left: Case 1 (instantaneous release filled LPG tank, 6500 m^3),Right: Case II (instantaneous release empty LPG tank, 438 m^3).

The position and the length of the flammable clouds are shown in the first two rows of Figure 4.2. The cloud position is defined as the centre location of the flammable cloud. Considering Case 1, the trailing and leading flammable clouds start to develop 66 s and 124 s after the rupture of the tank, respectively. The two clouds are not symmetrical due to the effect of the ventilation on the gas dispersion. The leading and trailing flammable clouds exit the tunnel at a time of 454 s and 563 s, respectively. The overpressure corresponding to the flammable cloud length at the different times is shown inFigure 4.2 c. The maximum overpressure (310 kPa) is reached when the trailing flammable cloud reaches the exit of the tunnel. The cumulative ignition probability of the flammable cloud is presented in Figure 4.2d for the two values $P_{single\ car}$. This graph shows that $P_{cumul} = 0.5$ when the

trailing flammable cloud reaches the end of the tunnel for $P_{\text{single car}} = 0.001$. In this case ignition in the tunnel occurs half of the time. For $P_{\text{single car}} = 0.007$ there is a cumulative probability of 1 that ignition occurs in the tunnel. The probability density function for both profiles is displayed in Figure 4-2 e. The same information is given for Case 2 in Figure 4.2f to j . The merging of the two flammable clouds produces a single cloud with a length of 80 m which coincides with the cloud length that generates a detonation wave. Therefore the overpressure sharply rises to the detonation overpressure when the two clouds merge.

It is possible to divide the complete cloud dispersion into a number of (sub)scenarios. Considering $P_{single\ car} = 0.007$ the cumulative ignition probability can be divided into 10 scenarios as shown in Figure 4.3. Each scenario has an equal ignition probability of 10%. For each scenario the corresponding flammable length of the cloud and the resulting overpressure are taken at the mid-point of the time interval. These results are listed in Table 4.2 for $P_{single\ car} = 0.001$. Some (sub)scenarios result in leading and trailing flammable clouds. For these cases the ignition probability is provided for each individual cloud (leading & trailing clouds, respectively). The equivalent results for the higher ignition probability $P_{single\ car} = 0.007$ are not given in this paper. It can however be observed from Figure 4.2 that at a higher ignition probability shorter clouds are more likely to be ignited resulting in lower overpressures.

The probability for the different scenarios for Case 2 are given in Table 4.3. The results clearly show that the gas explosion risks and consequences of an accident with an almost empty vessel is much higher than the accident with the full tank. This is a counter-intuitive outcome which is a direct consequence of the size of the explosive cloud formed in the tunnel (hence a result of the release and tunnel conditions).

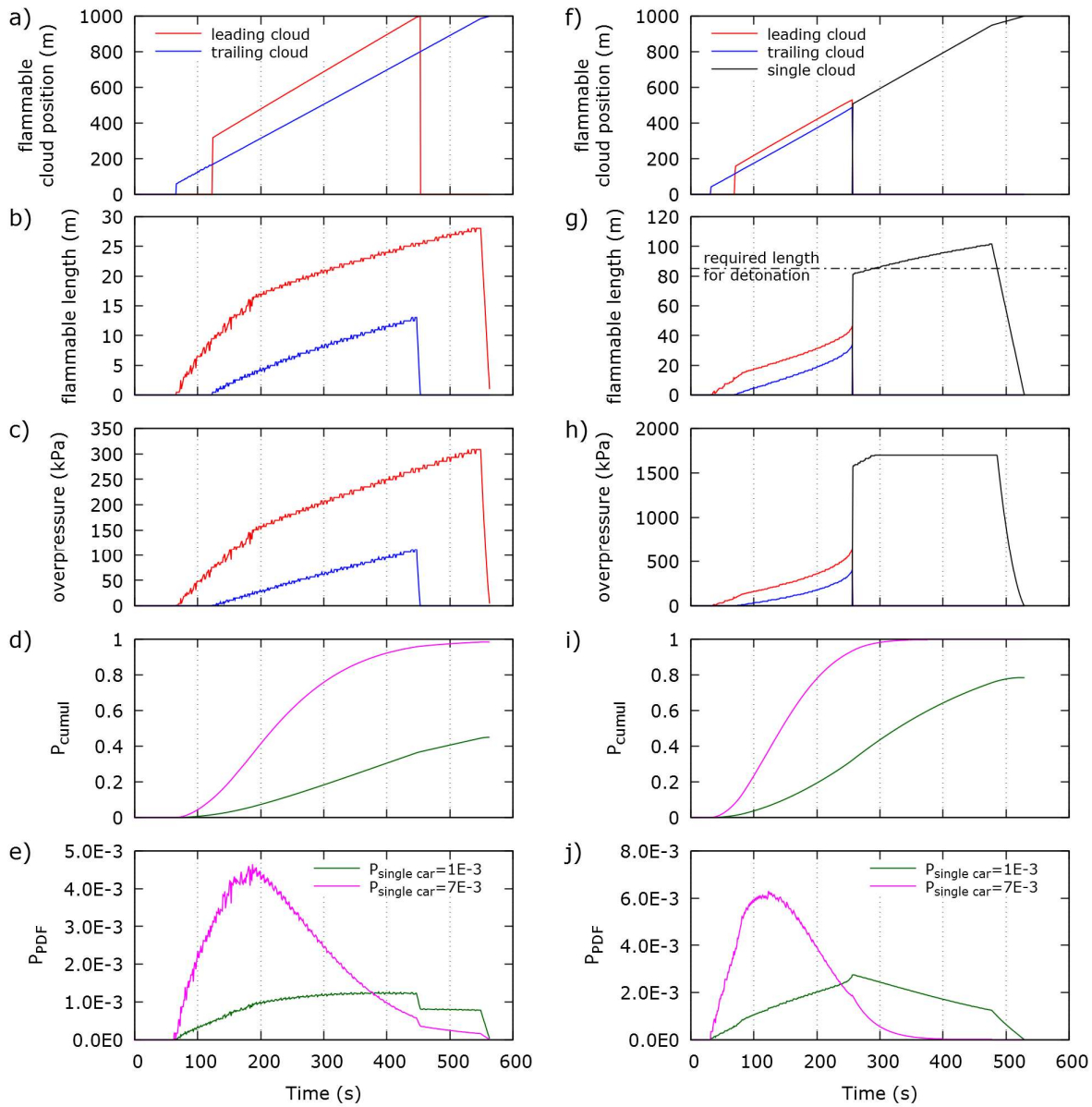

Figure 4.2 Flammable cloud position, flammable cloud length, overpressure, cumulative ignition probability and ignition probability density function for Case 1 Left (instantaneous release, 6500 m^3). Case 2 Right (instantaneous release, 438 m^3).

Table 4.2 Relative probability for different scenarios; Case 1 (instantaneous release, 6500 m^3) and $P_{single\ car} = 0.001$.

$P_{scenario}$ (10% bins; see Fig.4.3)	Leading flammable cloud Length (m)	Overpressure (kPa)	Trailing flammable cloud Length (m)	Overpressure (kPa)	Statistical parameters
10			8	61	
2.6 & 7.4	7	52	19.5	188	mean
3.1 & 6.9	10	81	22.5	228	
3.4 & 6.6	13	112	25	264	mode
5			27.5	301	
55	flammable cloud is outside of the tunnel without ignition				

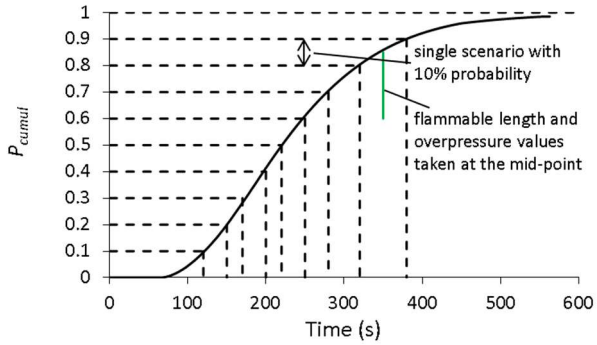

Figure 4.3 Division of the complete process into 10 (sub)scenarios for Case 1.

Table 4.3 Relative probability for different scenarios; Case 2 (instantaneous release, 438 m^3) and $P_{single\ car} = 0.001$.

$P_{scenario}$ (10% bins)	Leading flammable cloud Length (m)	Overpressure (kPa)	Trailing flammable cloud Length (m)	Overpressure (kPa)	Single flammable cloud Length (m)	Overpressure (kPa)	Statistical parameters
0.7 & 9.3	1	4	12.5	106			
3.5 & 6.5	15	134	27.5	301			
4.0 & 6.0	23.5	242	36	442			mean
10					82.5	1612	mode
10					87	1700	median
10					91.5	1700	
10					96	1700	
9					91	1700	
21	flammable cloud is outside of the tunnel without ignition						

4.3 Results Case 3

The evolution of the gas concentration for a continuous release of 15 kg/s is shown in Figure 4.4a. Approximately 435 s are required for the complete amount (12 500 kg) of liquid propane to leak out of the tank. Therefore the 100 s and 300 s profiles show the leading edge of the cloud, but it is only with the other profiles (500 s, 700 s and 900 s) that the trailing edge can be observed. The resulting mixture produced by a ventilation of 2 m/s and a liquid propane leak rate of 30 kg/s (or gaseous leak rate of 15 kg/s) is such that the gaseous fuel concentration is 5.4 % which is between the LFL and UFL boundaries. The flammable cloud length is therefore significantly greater than the previous cases and this can be observed in Figure 4.4c. Consequently the cumulative ignition probability increases rapidly and the peak of the probability density function is obtained soon after the start of the gas release as presented in Figure 4.4e and f.

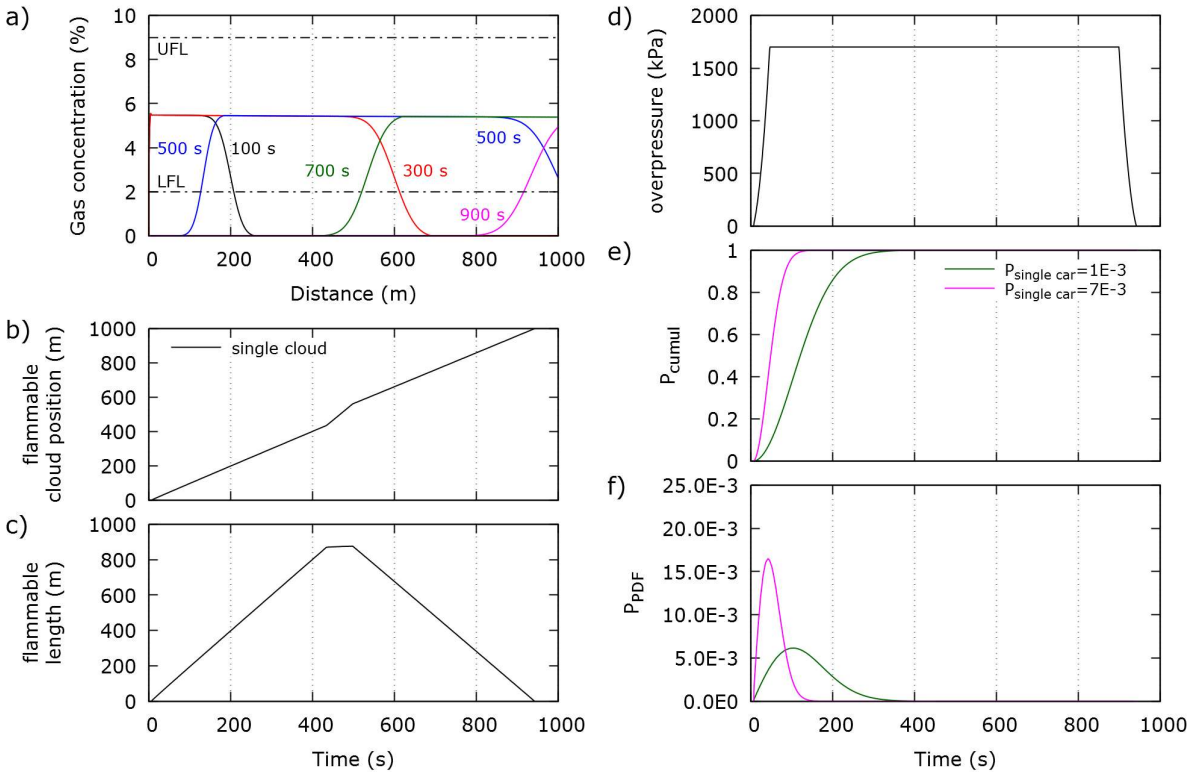

Figure 4.4 (a) Gas concentration profiles at different times for Case 3 (continuous release at 15 kg/s). (b-f) Flammable cloud position, flammable cloud length, overpressure, cumulative ignition probability and ignition probability density function for Case 3 (continuous release at 15 kg/s).

4.4 Results summary

The results of the three cases are summarized in Table 4.4 where the mode, median and mean overpressure values are provided for both $P_{single\ car} = 0.001$ and $P_{single\ car} = 0.007$. For the cases where two flammable clouds co-exist (such as Case 1), the cloud that generates the larger overpressure is considered for the mode, median and mean values. In general the overpressure levels from $P_{single\ car} = 0.007$ are lower than for $P_{single\ car} = 0.001$ for the same case. Furthermore the case of a continuous release provides the worst resulting overpressure levels.

Table 4.4 Mode, median and mean values for the different cases.

		Overpressure (kPa)		
	$P_{single\ car}$	Mode	Median	Mean
Case 1	0.001	264	N/A	188
(instant. release, 6500 m^3)	0.007	134	163	169
Case 2	0.001	1612	1700	442
(instant. release, 438 m^3)	0.007	188	221	256
Case 3	0.001	1700	1700	1700
(contin. release at 15 kg/s)	0.007	1290	1678	1700

5 CONCLUSIONS

A tunnel accident with a transport of flammable liquefied gases may result in a gas explosion after dispersion and delayed ignition. Quantification of the risk of this scenario is important to take informed decisions on tunnel design and routing of dangerous goods. In a risk analysis both the consequences and the probability of occurrence have to be considered. For this reason TNO has extended its model for dispersion and gas explosion overpressure with an ignition probability model.

The model has been illustrated with three case studies. In these case studies it has been assumed that the ventilation speed is in the direction of the traffic and that the ignition probability is dominated by vehicles. These assumptions together imply that the accident scenario of a truck driving into a traffic jam is the most relevant to consider. In this case the explosive cloud will potentially meet a large number of vehicles (ignition sources).

The case studies with an instantaneous LPG release show that the cloud is initially above the UFL. Subsequently the gas concentration either remains mostly fuel-rich by the time the cloud reaches the end of the tunnel or falls within the flammability limits before the tunnel exit, depending on the initial amount of fuel released. A case study with a continuous LPG release shows that depending on the release rate and the ventilation speed, the tunnel may be completely filled with a flammable mixture. The simulations provide the overpressure for different scenarios linked with their probability of occurrence. A higher basic ignition probability (per car per second), generally leads to lower overpressures. This is caused by the fact that for a higher basic ignition probability the cloud ignites earlier, at a time when the cloud is less developed.

The case studies clearly show the capability to quantify consequences and probabilities for various accident scenarios. The case studies also show that this level of detail is needed to make consistent predictions. The combination of the gas dispersion, gas explosion and ignition models are needed, to derive design loads for tunnels, to perform tunnel safety assessments, and to develop safety measures. They form the backbone for quantitative risk assessments.

Further research is recommended on the influence of vehicles on gas dispersion in tunnels, and the limitations of 1D gas dispersion models. Dispersion modelling solutions for extraction of fuel-air mixture at the tunnel ceiling, and changes in tunnel diameter and branching are of interest.

In order to make more reliable predictions of the ignition probability, the values of two relevant model parameters need to be validated. These parameters are the ignition probability of a single car which remains in a flammable mixture for one second, as well as the ignition delay time. For this purpose it is recommended to analyse ignition delay times observed in accidents, and to perform experiments with various types of vehicles in flammable clouds, while monitoring the time and location of ignition.
Furthermore a validation of the assumed flame speeds and run-up to detonation lengths for other car densities and fuels than those tested in the test campaign for the development of the explosion model is recommended.

6 REFERENCES

1. Van den Berg A.C., Rhijnsburger M.P.M. and Weerheijm J. (2001). *Vuistregels voor explosie-belasting en respons van verkeerstunnels*. TNO report no. PML 2001-C121 (in Dutch).

2. Van den Berg A.C. (2009). *"BLAST" - a compilation of codes for the numerical simulation of the gas dynamics of explosions*. Journal of Loss Prevention in the Process Industries, 22, (2009), pp.271–278
3. Van den Berg A.C. and Weerheijm J. (2010). *Towards an explosion-resistant tunnel structure: The design pressure load*. TNO report no. TNO-DV2010-IN484.
4. Van den Berg A.C. (2010). *Dispersion of large quantities of gas in long tunnel tubes*. TNO Defence, Security and Safety report.
5. Eckhoff, R.K., Ngo, M., Olsen, W. (2010). *On the minimum ignition energy (MIE) for propane/air.* J Hazard Mater. 2010 Mar 15;175(1-3):293-7. doi: 10.1016/j.jhazmat.2009.09.162. Epub 2009 Oct 9.
6. Hjertager B.H. et al. (1984). *Flame acceleration of propane-air in a large-scale obstructed tube.* Progress in Astronautics and Aeronautics,Vol.94,(1984),pp.504-522. AIAA Inc. 1984, New York
7. http://www.engineeringtoolbox.com/fuels-ignition-temperatures-d_171.html. Consulted on 21 November 2014.
8. Lee J.H.S. et al. (1984). *High speed turbulent deflagrations and transition to detonation in H2-air mixtures*. Combustion and Flame,Vol.56,(1984),pp.227-239
9. Lewis, B., von Elbe, Guenther. (1987). *Combustion, Flames and Explosions of Gases*. ISBN: 978-0-12-446751-4, June 1987.
10. De Maaijer M., Van den Berg A.C. en De Bruijn P.C.J. (2002). *Veiligheid Ondergrondse Infrastructuur Small-scale experiments and numerical simulation of gas explosions in tunnels*, TNO-Prins Maurits Laboratory report nr. PML 2002-IN18
11. Monin A.S. and Yaglom A M., (1971). *Statistical Fluid Mechanics: Mechanics of Turbulence.* The MIT Press, 1971
12. Schelkin K.I. and Troshin Ya.K. (1965). *Gasdynamics of Combustion*. Mono Book Corp., Baltimore, 1965.
13. Taylor G.I. (1954). *The dispersion of matter in turbulent flow through a pipe.* Proc.Roy.Soc. London A223,(1954),pp.446-468
14. Verreault, J., van der Voort, M.M., Weerheijm, J. (2014). *Probability of ignition of a fuel-air mixture in a tunnel*. TNO-2014-R11690, November 2014.
15. Wang Jifei, Huang H.W., Xie Xiongyao (2010). *The application of F&EI Method in Risk Assessment of Tunnel Gas Explosion*. GeoShanghai International Conference. May 2010. Doi:10.1061/41107(380)44
16. Weerheijm J. and Van den Berg A.C. (2014). "Explosion Risks and Consequences for tunnels" Proceedings ISTSS 2014, Marseille, March 2014, France.
17. Weerheijm, J., van der Voort, M.M., Verreault, J., Van den Berg, A.C. (2015). *Quantitative risk analysis of gas explosions in tunnels; probability, effects, and consequences*. 5th International Conference on Design and Analysis of Protective Structures, DAPS, Singapore, 19-21 May 2015.
18. Zalesak, S. T. (1979). *Fully multidimensional Flux-Corrected Transport algorithms for fluids*. Journal of Computational Physics, 31, 335–362.
19. Zang Qi, Qin Bin, Lin Da-Chao (2016). *A methodology to predict shock ovepressure decay in a tunnel produced by a premixed methane/air explosion*. Journal of Loss Prevention in the Process Industries, November 2016, Vol. 44: 275-281, doi:10.1016/j.jlp.2016.10.002

Annex A: BACKGROUND TNO GAS EXPLOSION MODEL FOR TUNNEL GEOMETRIES

A1 Modelling gas explosions

As described in section 2.1.1, a gas explosion is a process of intense interaction of three strongly interrelated phenomena: expansion flow, flow structure (viscosity and turbulence) and combustion. Its development is predominantly governed by the nature of the boundary conditions. In a model of a gas explosion, these three phenomena and their strong dependence on the boundary conditions should be adequately modelled. In the 1990's TNO developed the CFD codes ReaGas and AutoReaGas to simulate the explosion process, see [A3, A4]. In these 3D-CFD codes the gas dynamics of expansion is modelled by conservation equations for mass, momentum and energy. Turbulence and combustion rate are taken into account to represent the gas mixing, energy release and gas expansion. The code development was accompanied with extensive European experimental campaigns (e.g. MERGE, EMERGE, see ref [A5, A6]).

Based on the gained knowledge and expertise on reactive gas dynamics, the gas explosion process for tunnel geometries was simplified to a 1-dimensional numerical gas explosion model which has been developed for tunnel conditions. This development was also accompanied with test campaigns.

A 2 The one-dimensional gas explosion model [A1]

A vapour cloud explosion is a process of flame propagation through a flammable mixture of fuel and air. The gas dynamics of flame propagation may be simulated under one-dimensional geometry by moving an energy addition wave over a onedimensional numerical mesh. The wave of a few cells thick, which may be propagated at any desired flame speed, smoothly adds the heat of combustion to the gaseous material specified in the mesh. To this end, the energy conservation equation is provided with a source term that has been appropriately shaped to this end. In a one-dimensional mesh for a tunnel, the energy addition wave is propagated from the ignition location in longitudinal direction, see Figure A-1. The added energy depends on the position of the cell within the flame front. For cell i the cumulative added energy is:

$$\Delta E = \frac{a}{b}.Q \ ,$$

with Q = heat of combustion and b = thickness of the flame front.
Note that in the model atmospheric pressure is defined as boundary condition for the tunnel exits.

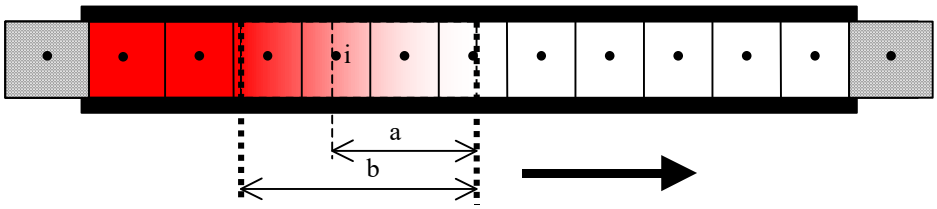

Figure A-1 One-dimensional numerical model of gas explosion in tunnel tube. Flame propagation modelled as flame-front (length of several cells) with prescribed velocity, in which the combustion heat is added gradually in time.

As soon as the energy addition process has started the gaseous material starts expanding and consequently starts moving relative to the mesh and the energy addition wave. The gas flow is described with the Euler equations for compressible gases, neglecting friction:

$$\frac{\partial \rho}{\partial t} + \frac{\partial}{\partial x}(\rho u) = 0$$

$$\frac{\partial}{\partial t}(\rho u_i) + \frac{\partial}{\partial x_j}\left(\rho u_j u_i\right) + \frac{\partial p}{\partial x_i} = 0$$

$$\frac{\partial}{\partial t}(\rho E) + \frac{\partial}{\partial x_j}\left(\rho u_j E\right) + \frac{\partial}{\partial x_j}(p u_j) = 0$$

With ρ = density (kg/m^3)
u = velocity of gas (m/s)
E = e + ½u^2 + F.Q (J/kg)
e = internal energy (J/kg)
p = pressure (Pa)
Q = heat of combustion (J/kg)
F = control parameter energy-addition (value 0 – 1)
x = coordinate (m)
t = time (s)

These equations make use of the convention that a summation should be carried out for terms in wich the index j occurs twice.

A proper energy addition process, which adds a fixed quantity of heat of combustion per unit mass of material, requires therefore the definition of a reactedness or reaction progress parameter *F*, defined as being the mass fraction reacted material in a cell. The value of *F* is used to control the energy addition to the expanding material. The reactedness *F* is made to vary smoothly from 0 (unburned) in front of the flame to 1 (burnt) behind the flame. The reactedness distribution is a material property and should as such be transported along with the expansion flow by the integration of an extra transport equation presented for the reactedness mass fraction:

$$\frac{\partial}{\partial t}(\rho F) + \frac{\partial}{\partial x}(\rho u F) = \frac{\rho}{\tau}$$

In which τ is the time of energy addition, which controls the thickness (number of cells) of the energy addition front. The ratio of specific heats of the medium γ is assumed to be proportional to *F*, varying from $\gamma_0 = 1.4$ for the unreacted gas mixture to $\gamma_1 = 1.25$ for the fully reacted gas mixture, so

$$\gamma = \gamma_0 - F(\gamma_0 - \gamma_1).$$

These values of the specific heat combined with the heat of combustion of 2.76 MJ/kg of stoichiometric propane air mixture, result in realistic expansion values.

In the compational model this set of equations is solved by means of a finite difference method based on a Flux-Corrected Transport (FCT) scheme (A2). As mentioned, the open tunnel exits are pesented as boundary conditions with atmospheric pressure. The computations result in pressure distribution along the tunnel axis as a function of time, i.e. $P(x,t)$.

Annex A References

A1 Berg, A.C. van den, (2009) ‘‘BLAST’’: A compilation of codes for the numerical simulation of the gas dynamics of explosions, Journal of Loss Prevention in the Process Industries 22

(2009) 271–278

A2 Boris J.P., (1976), Flux-Corrected Transport modules for solving generalized continuity equations. NRL Memorandum report 3237. Naval Research Laboratory,Washington,D.C.

A3 Centre for Chemical Process Safety, AIChE,7994 Century Dynamics/TNo (1998) AutoReaGas User Documentation. Version 2.0

A4 Fairlie G.E. (1998) AutoReaGas Modelling of Test Condition Variations in Full Scale Gas Explosions Centrny Dynamics Ltd. &, TNO-PML report for HSE oro 98 048, 1998

A5 Mercx W.P.M.,(1994) Modelling and Experimental Research into Gas Explosions Overall Final Report for the MERGE project CEC contract STEP-CT-O1 I 1(SMA)

A6 Mercx W.P.M.,(1996) Extended Modelling and Experimental Research into Gas Explosions Overall Final Report for the EMERGE project CEC contract EV5V-CT93 -027 4

Annex B: Dispersion according Taylor equation

B1 MODELLING OF GAS DISPERSION IN A LONG TUBE

B1.1 Theory of shear dispersion

Figure B1 simply illustrates the phenomenology of shear dispersion in a channel.

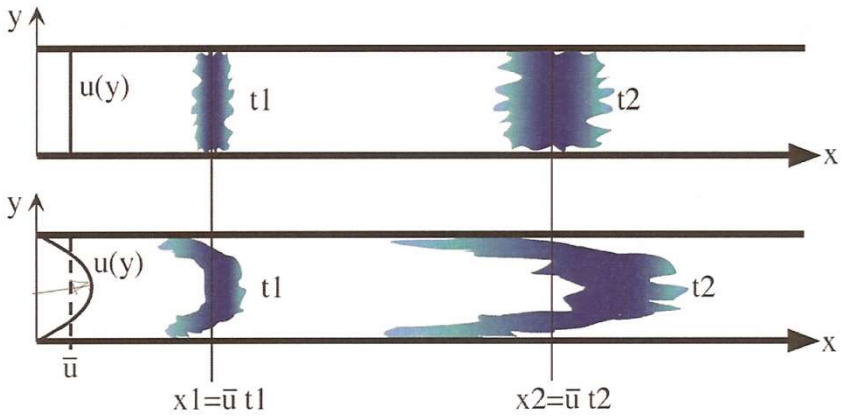

Figure B1 Phenomenology of shear dispersion in a channel.

The upper part of the figure shows a puff of material dispersing in a homogeneous flow field by turbulent or molecular diffusivity. The lower part shows the same puff of material, now dispersing in a flow field characterised by a flow velocity distribution. It shows how the concentration distribution deforms in the shear flow and and diffuses at the same time. The convective transport by the velocity distribution generates concentration differences over the channel's cross-section. At the same time the cross-sectional concentration differences are being smoothed by lateral diffusive transport. The interaction of the velocity distribution and lateral diffusive transport in a tube makes the dispersion process in longitudinal direction much faster than through diffusive transport in lengthwise direction alone. A long distance downwind of the source, the concentration differences over the tube's cross-

section are becoming smaller and smaller. The concentration distribution far downwind may therefore be considered approximately one-dimensional.

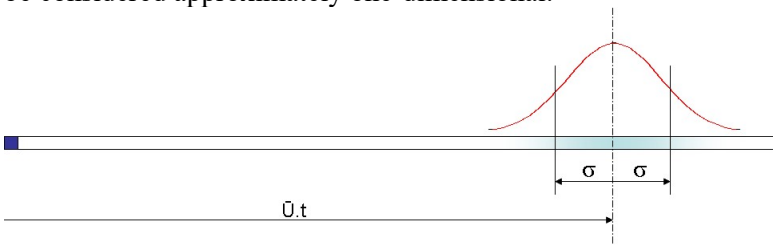

Figure B2 Normal concentration distribution far downwind of an instantaneous source in a long channel.

Experimental observations (Taylor, 1954) have shown that far downwind of the source the cross-sectionally averaged concentration is normally distributed in lengthwise direction approximately (Figure B2), that is mathematically:

$$\overline{C}(x,t) \approx \frac{Q}{A_t \sigma(x)\sqrt{2\pi}} EXP\left[-\frac{(x-\overline{U}t)^2}{2\sigma^2(x)}\right]$$

with

$$\sigma(x) = \sqrt{2K_{eff}t} = \sqrt{2K_{eff}\frac{x}{\overline{U}}}$$

where:

$\overline{C}$ = concentration averaged over the cross-section ($m^3.m^{-3}$)
Q = source strength (m^3)
A_t = tunnel cross-sectional area (m^2)
σ(x) = standard deviation of the normal distribution (m)
x = downwind distance (m)
$\overline{U}$ = flow velocity averaged over the cross-section ($m.s^{-1}$)
t = time (s)
K_{eff} = effective longitudinal dispersion coefficient ($m^2.s^{-1}$)

The one-dimensional normal concentration distribution in lengthwise direction is a solution of the one-dimensional dispersion equation:

$$\frac{\partial \overline{C}}{\partial t} + \overline{U}\frac{\partial \overline{C}}{\partial x} = K_{eff}\frac{\partial^2 \overline{C}}{\partial x^2}$$

The effective longitudinal dispersion coefficient K_{eff} is substantially larger than the molecular or turbulent diffusivity in lengthwise direction. Following Taylor (1954), the effective longitudinal dispersion coefficient K_{eff} can be derived from the multi-dimensional dispersion equation under the condition that a long way downwind of the source the concentration distribution has become approximately homogeneous over the channel cross-section. Then for a two-dimensional shear flow for instance, the longitudinal dispersion coefficient K_{eff} can be approximated from:

$$K_{eff} = -\frac{1}{H}\int_0^H (U(z)-\overline{U})dz \int_0^z \frac{dz'}{K_z(z')}\int_0^{z'}(U(z'')-\overline{U})dz''$$

where:

H = cross-flow dimension of the channel (m)

U(z) = flow velocity ($m.s^{-1}$)
$\overline{U}$ = cross-sectionally averaged flow velocity ($m.s^{-1}$)
K_z = cross-flow diffusivity ($m^2.s^{-1}$)
z,z',z'' = coordinate in cross-flow direction (m)

And for the shear flow in a tube of circular cross-section:

$$K_{eff} = -2R^2 \int_0^1 [U(z) - \overline{U}]z.dz \int_0^z \frac{dz'}{z' K_z(z')} \int_0^{z'} [U(z'') - \overline{U}]z''.dz''$$

where:

$z, z', z'' = \frac{r}{R}$ = cross-flow coordinate and R = tube radius

For simple well-defined shear flows, these expressions can be readily evaluated. For laminar flow pipe in a circular tube, where the cross-sectional velocity distribution is parabolic, the effective longitudinal dispersion coefficient can be analytically evaluated according (Taylor, 1954), as:

$$K_{eff} = \frac{\overline{U}^2 R^2}{48D}$$

where D is the molecular diffusivity of the fluid. For turbulent flow in a circular pipe and under appropriate assumptions for the cross-sectional turbulent diffusivity, K_{eff} can be numerically evaluated from experimental data on the cross-sectional flow velocity distribution. In this way, Taylor (1954) was able to approximate the effective longitudinal dispersion coefficient for turbulent pipe flow as:

$K_{eff} = 10.1 \times R \times u^*$

$$u^* = \sqrt{\frac{\sigma_w}{\rho}}$$

With u^* = wall friction velocity ($m.s^{-1}$)
σ_w = wall shear stress (Pa)
ρ = fluid density ($kg.m^{-3}$)
R = tube radius (m)

The wall friction velocity is roughly proportional to the flow velocity. The proportionality factor however, is a weak function of the Reynolds number (Re) of the flow and has been given by Taylor (1954) in graphic form. The graphical representation was analytically be approximated as:

$$\frac{U}{u^*} = 5.0 \times^{10} \log(\mathrm{Re}) - 3.83$$

Using the results of Taylor, schematizing the dispersion process in the tunnel according to the flow in a circular tube with an effective hydrodynamic diameter, the downwind concehtration due to an instantaneous release can also be derived.

B1.2 Downwind concentration distribution due to an instantaneous release

The one-dimensional normal concentration distribution in lengthwise direction, is:

$$\overline{C}(x,t) = \frac{Q}{A_t \sigma(t)\sqrt{2\pi}} EXP\left[-\frac{(x - \overline{U}t)^2}{2\sigma^2(t)} \right]$$

where :

$\overline{C}(x,t)$ = volume fraction distribution at time t ($m^3.m^{-3}$)

Q = source strength (m^3)

A_t = tunnel cross-sectional area (m^2)

$\sigma(t) = \sqrt{2K_{eff}.t}$ = standard deviation (m)

x = downwind coordinate (m)

K_{eff} = $10.1 \times R_H \times u^*$ ($m^2.s^{-1}$)

The concentration distributions at various distances downstream of an instantaneous release of a quantity of gas are found by evaluating the above normal distribution at various points of time. The normal distribution however, is based on the mathematical concept of an instantaneous release from a point source. Consequently, it behaves unrealistically in the vicinity of the source where it results in concentrations higher than 100% and running up to infinity in the source.

It is more elegant to evaluate an equivalent of the normal distribution, that is:

$$\overline{C}(x,t) = \frac{Q}{A_t.L}\left[erf\left(\frac{0.5L-(x-\overline{U}t)}{\sigma(\overline{U}t)}\right)+erf\left(\frac{0.5L+(x-\overline{U}t)}{\sigma(\overline{U}t)}\right)\right]$$

Q = source strength (m^3)

A_t = tunnel cross-sectional area (m^2)

L = initial cloud length = Q/A_t (m)

erf(y) = error function, defined as:

$$\frac{1}{\sqrt{2\pi}}\int_0^y EXP(-\frac{t^2}{2}).dt$$

The error function distribution describes the downwind concentration distribution due to an instantaneous release from a source of size L.
The initial concentration in the source area is equal to 1, that is 100%. The concentration distribution increasingly approximates a normal distribution for growing downwind distance.

As an example, the error function distribution has been evalutated at various points of time after the release of 500 m^3 gas and an average flow velocity of 3 m/s in a tunnel of 5 × 14.4. Figure B3 shows how the downwind distribution develops, dependent on a logarithmic downwind coordinate. Because the flammability of propane is of concern in this study, the flammability region of propane in air (2% - 9%) has been indicated.

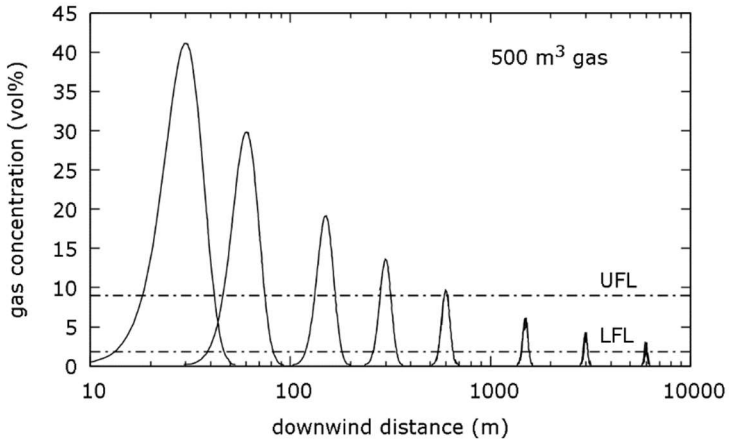

Figure B3 Consecutive concentration distributions downwind of an instantaneous release of 500 m^3 gas in a long tunnel tube (logarithmic downwind coordinate).

Figure B3 shows how the concentration distribution in a cloud of 500 m^3 LPG has developed at 10, 20, 50, 100, 200, 500, 1000, 2000 and 5000 s respectively after release. It shows how the concentration gradually falls relative to the flammability region of propane in air. Initially, two areas of a flammable composition on either side of the cloud are separated by an area of a composition too rich to be able to propagate a flame. Subsequently, when the maximum concentration falls down the upper flammability limit, there is one continuous area of a flammable composition. This has been demonstrated in Figure 2.3 of the main text. It shows how the flammability in the cloud after 100 s consists of two separated areas of 21 m length, developing into one single continuous area of 136 m length after 500 s.